Synergy of Electronic Excitations and Elastic Collision Spikes in Sputtering of Heavy Metal Oxides

T. Schenkel, A. V. Barnes, A. V. Hamza, and D. H. Schneider
Lawrence Livermore National Laboratory, Livermore, California 94550

J. C. Banks and B. L. Doyle
Sandia National Laboratory, Albuquerque, New Mexico 87185-1056
(Received 15 December 1997)

The emission of secondary ions and neutrals from uranium oxide has been measured for impact of highly charged, heavy ions. Total ablation rates and secondary ion yields increase strongly with projectile charge. The dependencies on projectile charge ($16 < q < 70$), impact energy (10 keV $< E_{\mathrm{kin}} <$ 1 MeV), and projectile mass of secondary ion yields demonstrate the presence of an interaction regime where electronic excitation by charge neutralization and elastic collision spikes combine synergistically. [S0031-9007(98)06056-6]

PACS numbers: 79.20.Rf, 34.50.Fa

Sputtering and secondary ion emission from solids interacting with energetic particles are active research fields of great fundamental and applied interest. Momentum transfer to target atoms can be accomplished through elastic collisions or electronic processes. Linear collision cascade theory [1] has been used most successfully in describing the sputtering of metals by ions of keV energies. Enhancements due to elastic collision spikes are observed when both projectile and target consist of very high Z materials [2]. At energies of several hundred keV, close to the nuclear stopping maximum, sputtering yields increase due to nonlinear effects as most atoms in the spike volume are set into motion. Controversial discussions have evolved on the nature of sputtering mechanisms in the interaction of slow, highly charged ions with solids [3–8]. Defect mediated sputtering has been demonstrated for some alkali halides and SiO_2 [3] bombarded by slow Ar^{q+} ($q \leq 14$) and Xe^{q+} ($q \leq 27$). Sputtering through collective excitation mechanisms such as Coulomb explosions accompanied by shock waves was inferred from observations of high yields of atomic and cluster ions for very high projectile charge states ($q > 30$) [4,5,8]. Up to now, total sputter yields of materials were known only for impact of ions with charge states $q \leq 27$ (for Xe).

In this Letter we report on the first measurements of total sputtering and secondary ion yields from uranium oxide interacting with slow, highly charged, heavy ions with charge states up to 70+. Here, a new ion-solid interaction regime, where projectile charge and momentum are both critical, is observed. In this regime, electronic excitation by neutralization of highly charged ions and elastic collision spikes combine to produce a synergistic enhancement of secondary particle emission.

We used the catcher target technique [6] to determine total sputtering yields. Secondary ion yields were measured by time-of-flight secondary ion mass spectrometry (TOF-SIMS) [4,8]. Highly charged ions (HCI) were extracted from the electron beam ion trap (EBIT) at Lawrence Livermore National Laboratory. The experimental setup for ion extraction and TOF-SIMS has been previously described [4,8]. Polycrystalline uranium (^{238}U) targets were prepared by electropolishing followed by oxidation in air for several hours for native oxide formation. The oxide thickness was estimated from known oxidation rates [9] to be several hundred nanometers. Targets were cleaned after insertion into vacuum by low energy ion sputtering. The pressure in the target chamber was kept below 5×10^{-10} torr. Surface conditions were monitored closely by TOF-SIMS. Secondary ion spectra were reproducible over several sputter cleaning cycles. No charging of thin insulating layers was observed. For total sputter yield measurements, projectiles impinged on the targets at an incident angle of 30° relative to normal. SiO_2 (150 nm thick thermal oxide on Si) catcher targets were placed in parallel to the sputter target at a distance of 6 mm. Secondary neutrals and ions emitted from uranium oxide during exposure were collected on the catcher target. Typically highly charged ion fluxes were $\sim 10^5$ ions/s for Au and $\sim 10^6$ ions/s for Xe ions. Accurate determination of the HCI flux is crucial for our experiment. The flux was determined by single ion pulse counting of projectiles impinging on a microchannel plate detector (MCP). Bias voltages and discrimination levels in counting electronics were carefully set to assure constant detection efficiencies for ions of all charge states and impact energies [10]. Fluences ($\leq 10^6$ ions/s/cm^2) were well below critical levels for complete channel recovery in MCPs [10]. The MCP used for direct detection of HCIs was calibrated by single ion counting in a Daly detector arrangement. The strong burst of secondary electrons emitted by individual HCIs incident on solid targets allows for detection of HCIs with 100% efficiency [4,8]. The efficiency of the MCP for direct detection of HCIs was 0.61 ± 0.02. More details will be given in a forthcoming publication [11]. The flux was

measured every few hours during exposures. Ion doses were calculated from measured fluxes, exposure times, and the detection efficiency of the MCP. HCI beams from EBIT were stable over long periods, and dose uncertainties due to flux instabilities were typically $<10\%$. Doses ranged from 2×10^{10} (Au^{63+}) to 3×10^{11} (Xe^{27+}). Accumulation times were several days. Resulting surface coverages of ^{238}U on the catchers were $\sim 10^{11}$ atoms/cm^2. Ultralow coverages of heavy elements on light substrates can be determined quantitatively only by extremely sensitive surface analysis techniques. We used the heavy ion backscattering (HIBS) system at Sandia National Laboratory to determine uranium coverages *ex situ* [12]. The HIBS sensitivity for detection of uranium on otherwise clean silicon is $<10^9$ atoms/cm^2. Additionally, catcher targets could be analyzed *in situ* by highly charged ion based TOF-SIMS [4]. Sputter yields were calculated from surface coverages of uranium on the catchers, the ion dose, the view factor [13], and the sticking probability of uranium atoms on the catcher surface. The latter was assumed to be >0.9, similar to values found for uranium sticking on Al_2O_3 [6]. Assumptions on the currently unknown angular distribution of sputtered particles must be made when calculating the view factor of the catcher targets. This uncertainty translates into an uncertainty of total sputter yield values of $\sim 50\%$.

A typical TOF-SIMS spectrum recorded for Au^{69+} (220.8 keV) impinging on a uranium oxide target is shown in Fig. 1. The number of $(UO_x)^+_{n=1}$ counts ($x = 0, 1, 2, 3$) detected per incident ion is 37%. Only 8.45×10^5 Au^{69+} projectiles impinged on the target for the accumulation of this spectrum. Cluster ions with up to $n = 7$ uranium atoms could be detected.

Total ablation rates (open squares) are shown, together with positive secondary ion and cluster ion yields, as a function of incident ion charge q in Fig. 2(a). For total yield measurements, incident ions were $Xe^{27,44+}$, $Au^{62,63+}$, and Th^{70+} at impact velocities of $0.3v_{\mathrm{Bohr}}$. The relative error in the total yield data is $\sim 15\%$ resulting from uncertainties in HIBS results, ion dose measurements, and relative variations of view factors. Also shown are sputtering yields of uranium oxide for singly charged xenon and thorium ions at $0.3v_{\mathrm{Bohr}}$ as calculated by TRIM [14]. Sputtering yields of uranium oxide increase slightly with q for highly charged xenon ions. The increase by more than a factor of 2 when highly charged Au and Th ions interact with the target can result both from electronic sputtering at higher q and from increased momentum transfer due to the formation of elastic collision spikes in the target.

For measurements of secondary ion production, incident ions were Xe^{17-52+} (open triangles) and Au^{36-69+} (solid triangles). Here, the impact velocity was kept constant at $0.2v_{\mathrm{Bohr}}$. The error in secondary ion production rates is statistical and amounts to $<5\%$ of the rate value. The values reported here are secondary ion counts detected per incident projectile. For determination of total secondary ion yields, the detection efficiency of the spectrometer η must be known. Considering the detection efficiency

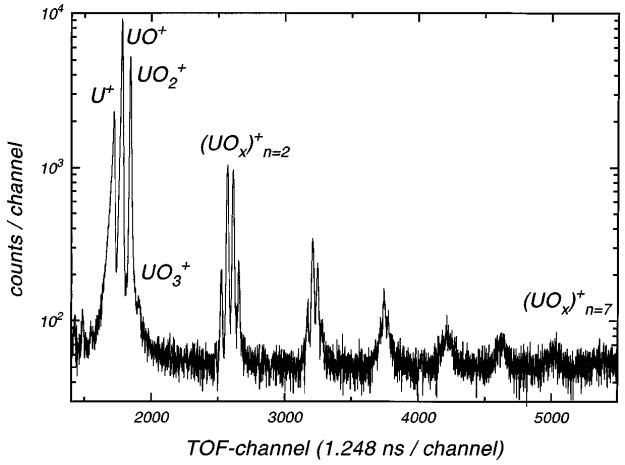

FIG. 1. TOF-SIMS spectrum of uranium oxide at impact of Au^{69+}.

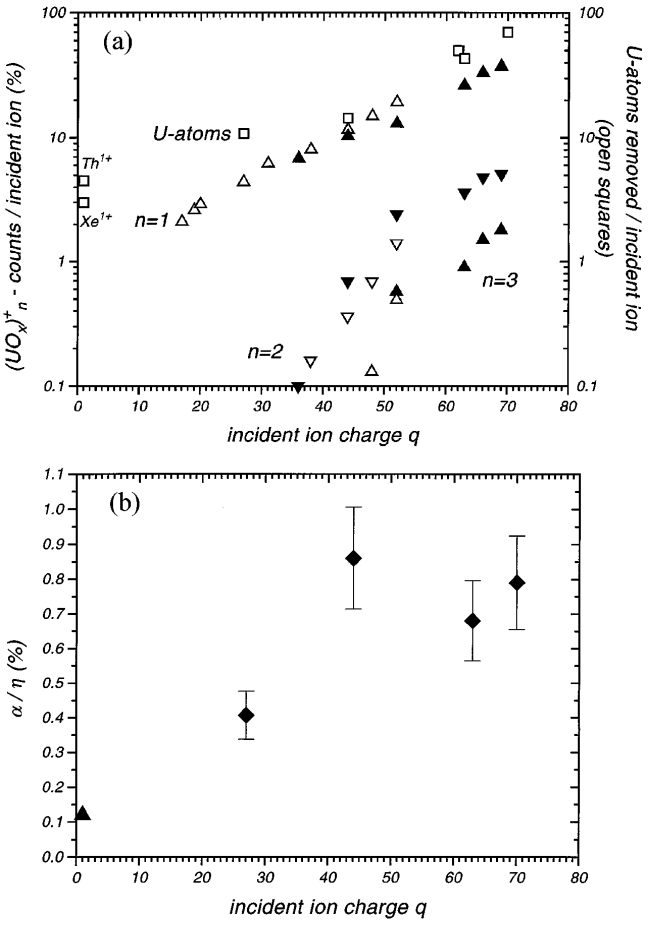

FIG. 2. (a) Total sputtering yield of U atoms (open squares), $(UO_x)^+_n$, $n = 1, 2, 3$, secondary ion production from uranium oxide and (b) ionization probability α for uranium ions as a function of projectile charge q. The detection efficiency for secondary ions η is $\sim 0.1-0.15$.

for secondary ions in the MCP [15] and the geometry with annular detector, we estimate η to be $\sim 0.1-0.15$. $(UO_x)_n^+$ yields, $n = 1, 2, 3$, increase strongly with q. At $q = 44$ and 52, the higher potential energy of the xenon ions ($E_{\text{pot}}[Xe^{52+}] = 121$ keV; $m = 136$ u) dominates for $n = 1$ over the higher momentum brought into the target by the gold ions ($E_{\text{pot}}[Au^{52+}] = 57.6$ keV; $m = 197$ u). This ratio is reversed for the emission of cluster ions $n = 2, 3$, where the influence of momentum dominates and cluster yields are higher for Au than for Xe projectiles. We attribute this to the development of elastic collision spikes in the target when bombarded with gold ions with energies of several hundred keV, near the nuclear stopping maximum [1,2]. Xenon ions are too light to form strong elastic collision spikes in uranium oxide.

Having measured both total sputtering yields and secondary ion yields, we can now for the first time determine the ionization probability for secondary ions emitted from a solid interacting with very highly charged ions. The ionization probability α is defined here as the number of positively charged uranium ions emitted per sputtered uranium atom. Yields of uranium ions from all species, $(UO_x)_n^+$, were added and divided by the number of uranium atoms removed per incident ion. The charge dependence of α, normalized to the detection efficiency η, is shown in Fig. 2(b). The data point at charge $q = 1$ gives an estimated upper limit of α for Xe^{1+} projectiles using the ion yield measured for Xe^{17+} and the total sputter yield from Xe^{27+}. For $q = 70$, ion yields from the impact of Au^{69+} were normalized to total yields for Th^{70+}. The impact velocity was $0.3v_{\text{Bohr}}$ in neutral and ion yield measurements for all projectiles. α is found to increase by a factor of 2 from Xe^{27+} to the highest charge state ions. In previous measurements of secondary ions and neutrals emitted from Si [7] and LiF [3] using multiply charged Ar ions ($q \leq 9$), values of α ranged from 0.01% to 0.1% and this finding was used to support a model of defect mediated sputtering [3]. The values reported here are more than an order of magnitude higher. This is the case even for the most conservative estimate of η, where collection of all secondary ions in the detector has to be assumed, and η is given by the detection efficiency of the MCP for ions with $m \geq 238$ u and $E_{\text{kin}} = 3.5$ keV of ~ 0.5 [15].

A characteristic signature of elastic collision spikes is the dependence of secondary neutral particle and ion emission on projectile energy. We have measured secondary ion yields as a function of kinetic energy for Xe^{27+}, Xe^{44+}, Au^{63+}, and Au^{69+} (Fig. 3). Ion yields vary only very weakly for xenon projectiles when the impact energy is increased from 20 to 500 keV. The yield dependence for Au^{63+} displays some structure with a weak maximum. The data for Au^{69+} show a pronounced maximum at ~ 220 keV. This energy value coincides with observations in elastic collision spike sputtering [2], where the maximum sputter yield is achieved at energies slightly below

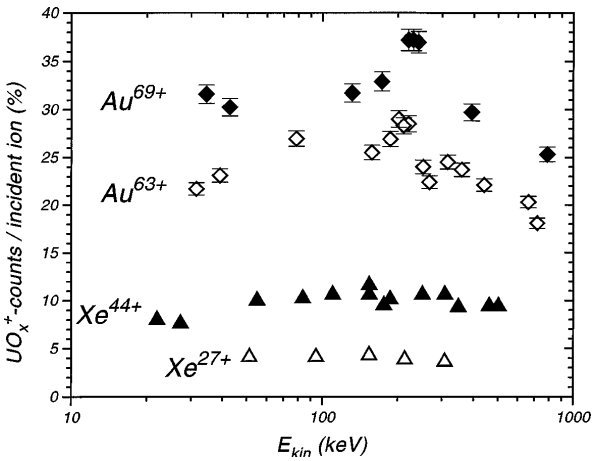

FIG. 3. Energy dependence of secondary ion production from uranium oxide at impact of Au^{69+}, Au^{63+}, Xe^{44+}, and Xe^{27+}.

the projectile energy corresponding to the nuclear stopping power maximum. The latter is reached at an energy of ~ 600 keV for singly charged gold ions in uranium oxide [14]. The finding of a more pronounced maximum in secondary ion emission for a more highly charged projectile demonstrates the critical interplay of projectile momentum and charge. For Au^{63+} ($E_{\text{pot}} = 122.3$ keV), the combination of high charge and momentum yields a weak but significant increase in secondary ion emission at elastic collision spike energies. For Au^{69+} ($E_{\text{pot}} = 168.6$ keV), the additional electronic excitation energy creates a condition above critical in both charge and momentum, and electronic sputtering through charge neutralization and elastic collision spikes combine synergistically. Increasing or decreasing the impact energy decreases momentum transfer below critical values for spike formation and yields drop similarly as observed in pure elastic spike sputtering. While conditions for elastic collision spikes are lost, electronic excitation through charge neutralization keeps secondary emission levels high.

Our results demonstrate the interplay of momentum transfer and electronic excitation in sputtering and secondary ion production from uranium oxide interacting with highly charged ions. For the component of electronic excitations, potential sputtering through decay of self-trapped excitons (STE) was demonstrated for LiF and SiO_2 bombarded by slow Ar^{q+} ($q \leq 14$) and Xe^{q+} ($q \leq 27$) [3]. Interestingly, strong potential sputtering with a pronounced dependence on charge does not always occur when STE can be produced in a material, as shown in Ref. [6] for CsI and Ar^{q+} ($4 \leq q \leq 11$). To our knowledge, formation of STE has not been reported for uranium oxides. A collective model of electronic sputtering is the Coulomb explosion model [16,17].

Time scales and energy dissipation mechanisms in the interaction of heavy, highly charged ions with heavy metal oxides can be described qualitatively in the following way. Slow, highly charged ions incident on solids relax via

formation of hollow atoms [8,18]. Hundreds of mostly low energy electrons, as well as photons and x rays, are emitted in the course of deexcitation. Momentum transfer to target electrons and nuclei is increased over values for singly charged ions due to charge state dependent stopping power contributions [19]. The potential energy of the ion is dissipated and charge state equilibrium is established after only a few femtoseconds (<10 fs) [5,19]. The slowdown time of Au^{63+} at 440 keV in uranium oxide is ~ 150 fs. During this time, collision cascades develop in the target. In the elastic collision spike regime, most target atoms are set into motion in the spike volume V_s, determined by the ranges of projectiles and recoils [1]. For Au ions at 440 keV, V_s is $\sim \pi (50\ \mathrm{nm})^3$. Spike lifetimes have been estimated to exceed slowdown times by orders of magnitude [2]. Coulomb repulsion between ionized target atoms in the charged domain causes the expansion of the near surface volume on the time scale of lattice motion of several hundred femtoseconds. This expansion can send a shock wave into the surrounding material. Positively charged atomic ions are emitted mostly from the core impact region, where the ionization density is highest. Heavy clusters are desorbed from a halo surrounding the core when the shock wave intersects the surface. Now, additional momentum can be added to expanding atoms and ions by energetic recoil atoms from the spike. At very high projectile charges and for very heavy projectiles interacting with heavy metal oxides, conditions for two nonlinear excitation mechanisms can both be met. The degree of target ionization in the impact center and the time scale for reneutralization by target electrons are not known, and existing theory does not provide much insight into the details of the interaction. The absence of noticeable yields of multiply charged positive secondary ions and ionization probabilities of $\sim 5\%-7\%$ indicate an ionization density of much less than one positive charge per target molecule at a time ~ 1 ps after HCI impact. Investigation of conditions of high defect densities [20] might resolve some of the controversy between models assuming decay of individual defects [3] and models of collective excitation such as Coulomb explosions [16,17].

In summary, we have measured secondary ion and total sputter yields from uranium oxide as a function of projectile charge and kinetic energy for highly charged, heavy ions. The interplay of charge and momentum opens a new ion-solid interaction regime, where elastic collision spikes and intense electronic excitation combine synergistically. For the electronic contribution to sputtering and secondary ion emission, the presence of collective mechanisms is indicated by the emission of heavy cluster ions and relatively high ionization probabilities for secondary ions.

The authors gratefully acknowledge the excellent technical support at the LLNL EBIT facility provided by D. Nelson and K. Visbeck. This work was performed under the auspices of the U.S. Department of Energy by Lawrence Livermore National Laboratory under Contract No. W-7405-ENG-48.

[1] P. Sigmund, in *Inelastic Ion-Surface Collisions*, edited by N. H. Tolk, J. C. Tully, W. Heiland, and C. W. White (Academic Press, New York, 1977), p. 128.
[2] H. L. Bay, H. H. Anderson, W. O. Hofer, and O. Nielsen, Nucl. Instrum. Methods Phys. Res. **132**, 301 (1976); P. Sigmund, Appl. Phys. Lett. **25**, 169 (1974); *ibid.* **27**, 521 (1975).
[3] T. Neidhart, F. Pichler, F. Aumayr, H. P. Winter, M. Schmidt, and P. Varga, Phys. Rev. Lett. **74**, 5280 (1995); *ibid.*, Nucl. Instrum. Methods Phys. Res., Sect. B **98**, 465 (1995); M. Sporn, G. Libiseller, T. Neidhard, M. Schmid, F. Aumayr, H. P. Winter, P. Varga, M. Grether, D. Niemann, and N. Stolterfoht, Phys. Rev. Lett. **79**, 945 (1997); P. Varga *et al.*, Phys. Scr. **T73**, 307 (1997).
[4] T. Schenkel *et al.*, Nucl. Instrum. Methods Phys. Res., Sect. B **125**, 153 (1997); T. Schenkel *et al.*, Mater. Sci. Forum **248-249**, 413 (1997).
[5] T. Schenkel *et al.*, Phys. Rev. Lett. **78**, 2481 (1997).
[6] D. L. Weathers, T. A. Tombrello, M. H. Prior, R. G. Stokstad, and R. E. Tribble, Nucl. Instrum. Methods Phys. Res., Sect. B **42**, 307 (1989); K. G. Liebbrecht, J. E. Griffith, R. A. Weller, and T. A. Tombrello, Radiat. Eff. **49**, 195 (1980).
[7] S. T. de Zwart, T. Fried, D. O. Boerma, R. Hoekstra, A. G. Drentje, and A. L. Boers, Surf. Sci. **177**, L939 (1986).
[8] D. H. Schneider and M. A. Briere, Phys. Scr. **53**, 228 (1996), and references therein.
[9] G. W. McGillivray, D. A. Geeson, and R. C. Greenwood, J. Nucl. Mater. **208**, 81 (1994).
[10] M. P. Stockli and D. Fry, Rev. Sci. Instrum. **68**, 3053 (1997).
[11] T. Schenkel, A. V. Barnes, A. V. Hamza, and D. Schneider (to be published).
[12] J. A. Knapp, D. K. Brice, and J. C. Banks, Nucl. Instrum. Methods Phys. Res., Sect. B **108**, 324 (1996).
[13] A. J. Chapman, *Heat Transfer* (Macmillan, New York, 1974), 3rd ed.
[14] J. Biersack, Nucl. Instrum. Methods Phys. Res., Sect. B **27**, 21 (1987).
[15] J. Oberheide, P. Wilhelms, and M. Zimmer, Meas. Sci. Technol. **8**, 351 (1997).
[16] I. S. Bitensky and E. S. Parilis, J. Phys. C **50**, 227 (1989), and references therein.
[17] H. P. Cheng and J. D. Gillaspy, Phys. Rev. B **55**, 2628 (1997).
[18] A. Arnau *et al.*, Surf. Sci. Rep. **229**, 1 (1997).
[19] T. Schenkel *et al.*, Phys. Rev. Lett. **79**, 2030 (1997).
[20] P. Stampfli, Nucl. Instrum. Methods Phys. Res., Sect. B **107**, 138 (1996).